# Detection of severe sliding and pitting fatigue wear regimes through the use of broadband acoustic emission

**E D Price**[1], **A W Lees**[1]*, and **M I Friswell**[2]
[1]School of Engineering, University of Wales Swansea, Swansea, UK
[2]Department of Aerospace Engineering, University of Bristol, Bristol, UK

*The manuscript was received on 7 November 2003 and was accepted after revision for publication on 17 January 2005.*

DOI: 10.1243/135065005X9817

**Abstract:** Acoustic emission techniques have been used to monitor severe sliding and pitting fatigue processes during four-ball testing. Results are presented that arose from a collaborative programme between the Naval Research Laboratory (Washington, DC) and the University of Wales Swansea, sponsored by the US Office of Naval Research. The ultimate aim of the research is to develop a systematic fusion technology approach to condition-based maintenance of wear-related surface distress of critical components in naval air and surface combatant engine and transmission systems. The principal monitoring technique utilized in this investigation was acoustic emission (AE). A custom data acquisition system was developed using a novel approach to collect AE signals. Post-test analysis of the data, in the frequency domain, demonstrates the advantage of analysing continuous AE and not just AE pulses.

**Keywords:** acoustic emission, sub-surface cracks, fatigue, scuffing, severe sliding, rolling element bearings, condition monitoring

## 1 INTRODUCTION

Recent advancements in machinery operational performance have placed increased demands on the components within these systems. When machinery is operated at the upper bounds of the performance envelope, failures often occur. In an effort to reduce such failures, many organizations responsible for machine maintenance are moving away from regular service intervals in favour of a more condition-based maintenance strategy.

For an effective condition-based maintenance strategy, the lead time to failure must be sufficient to allow the machine to be withdrawn from service without inconvenience. Many and varied condition monitoring techniques have been developed in recent years and although these systems are able to detect faults such as severe surface damage, the time between first detection and the fault progressing to a point at which the machine is no longer suitable for operation is often inadequately short. To increase lead times, damage must be detected at an earlier stage and fault progression accurately monitored.

As part of the US Navy transition initiative towards condition-based maintenance and machinery health prognostics, the US Office of Naval Research has recently funded research programmes to investigate the relative advantages of different condition monitoring techniques. The research programme conducted at the University of Wales Swansea was concerned with the fusion of vibration, acoustic emission (AE) and wear debris data from wear modes commonly experienced by gear and bearing components in naval air and surface combatants. The primary modes of failure in transmission systems are pitting fatigue and scuffing wear. A four-ball lubricant test machine was used to simulate these two wear modes during all experiments. During the research programme many interesting observations were made in the field of AE using a custom monitoring system and these are presented herein.

*Corresponding author: School of Engineering, University of Wales Swansea, Singleton Park, Swansea SA2 8PP, UK. email: a.w.lees@swansea.ac.uk

Acoustic emissions are high-frequency, transient waves emitted when changes in the microstructure of materials [**1**]. These stress waves can be detected by coupling piezo-electric transducers to the surface of the material under load [**2**]. Figure 1 shows the three main modes of AE generation.

Several commercial systems that are available to monitor acoustic emissions rely on a similar detection strategy [**3**]. The output from the transducers is continually monitored for any activity that exceeds a predefined threshold level. Once the signal level crosses the threshold, a hit is said to be detected and this can then be recorded or processed to extract information such as amplitude, duration, rise time, and so on (Fig. 2). Both burst and mixed modes of generation lend themselves well to detection with these systems as pulses can readily be identified, but if the pulse generation is so rapid that the signal appears continuous then a different approach is necessary.

With rotating machinery, exclusive burst mode activity is not seen, as there are often high levels of background noise. Healthy rotating machinery will typically emit AE continuously, with faults such as pitting appearing as bursts superimposed on the continuous signal, that is, mixed mode. Many have demonstrated the ability of AE to detect faults such as pitting in bearings, but the lead time to failure of these systems is highly dependent on the level of the background signal [**4**–**12**]. Bursts from early wear events can be buried in noisy environments. To monitor wear at an early stage and to better understand AE generation in rotating machinery requires the analysis of continuous AE.

The following sections describe the custom AE data acquisition system and the experimental apparatus used during the experiments. A comprehensive test programme was completed, yielding many results, a representative selection of which are included in this paper. These results are discussed in the later sections.

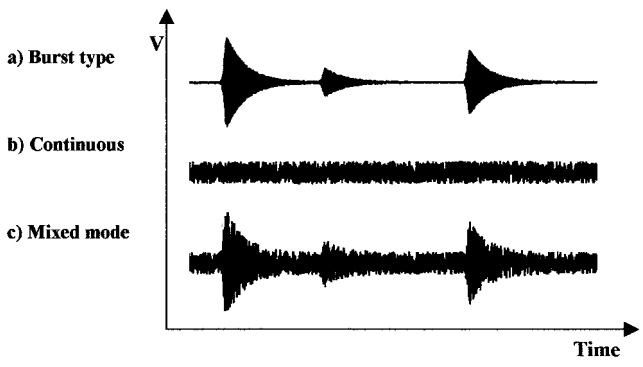


**Fig. 1** Different AE signal types

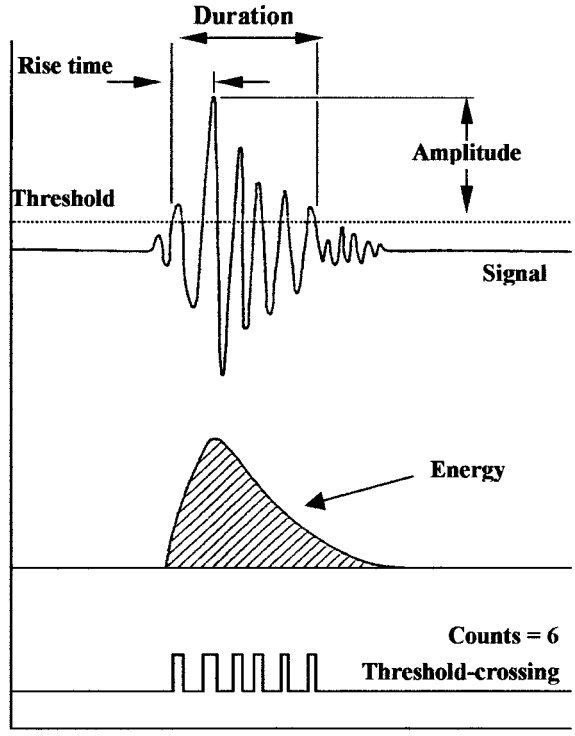


**Fig. 2** Acoustic emission pulse parameters

## 2 TEST EQUIPMENT

This section describes the experimental apparatus used in the laboratory, and looks in detail at the four-ball machine and how it was used to generate data from known wear regimes (Fig. 3).

The four-ball machine is normally utilized to perform lubricant tests according to internationally recognized standard test procedures [**13**]. In the UK, the designated standards are stipulated according to the Institute of Petroleum (IP) as follows: scuffing tests (sliding), IP239; pitting fatigue (rolling), IP300.

Figure 4 shows schematically the four-ball configurations for sliding (a) and rolling (b), respectively. The laboratory four-ball machine was a modification of the standard Stanhope-Seta IP239/97 machine, designed for the study of accelerated wear tests. Instead of an AC 1500 rpm motor there was a variable speed DC motor. This allowed the spindle speed to be varied from 500 to 3000 rpm. The loading was dependent on the type of test carried out. In the case of the severe sliding or scuffing test the load ranged from 36 to 150 kg. In the case of the pitting fatigue tests, the load range used was from 500 to 800 kg.

For sliding operation, the three lower balls were clamped in place and the upper fourth ball was rotated against them. For rolling contact, the lower three balls were free to rotate on their own axes

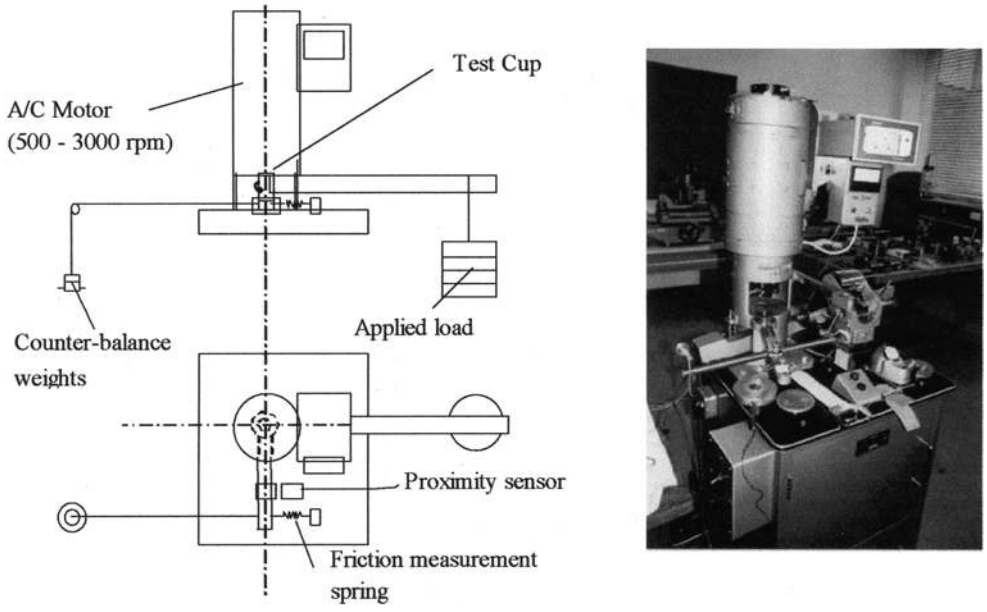


**Fig. 3** Four-ball machine

and around the 'race' cup under the driving action of the rotating upper ball. The geometry of the race was such that the orbit of each of the lower balls was random. As only the upper ball undergoes repeated cyclic loading on the same track, the upper ball should pit before the lower balls. All the balls used in the tests were 12.7 mm in diameter.

Sliding contaft tests were carried out, each for one minute, using applied loads in the range 36–150 kg, depending on oil type. As the load was increased incrementally with each successive test, non-additive, lower grade oils caused the upper ball to weld to the lower balls and the test was immediately discontinued. Wear was determined in accordance with IP239 procedures in that the average wear scar diameter was determined from two measurements at right angles to each other, (using an optical microscope) on each of the lower balls (six measurements in all). For the rolling contact mode tests, the running time to the formation of a pit in the upper ball was the sole criterion. Running times per test varied between a few minutes to about three hours. The applied load was in the range 500–800 kg. Lubrication was achieved by means of a simple oil bath that is the cup, which held approximately 9 mL of oil. The oil bath temperature rise was monitored and recorded using a K-type thermocouple embedded in the base of the cup. All loads quoted are those applied to the balls. The loading arm had variable mechanical advantage and a combination of this and the load on the loading arm were used to set the load at the contact (i.e. 20 to 1 mechanical advantage with 40 kg load gives 800 kg).

Throughout the severe sliding tests friction was also monitored. The amount of friction force generated by the rotation of the spindle on the three lower balls was calculated by measuring the movement of the clamp arm, which was being restrained by a spring of known stiffness. A pre-load is applied

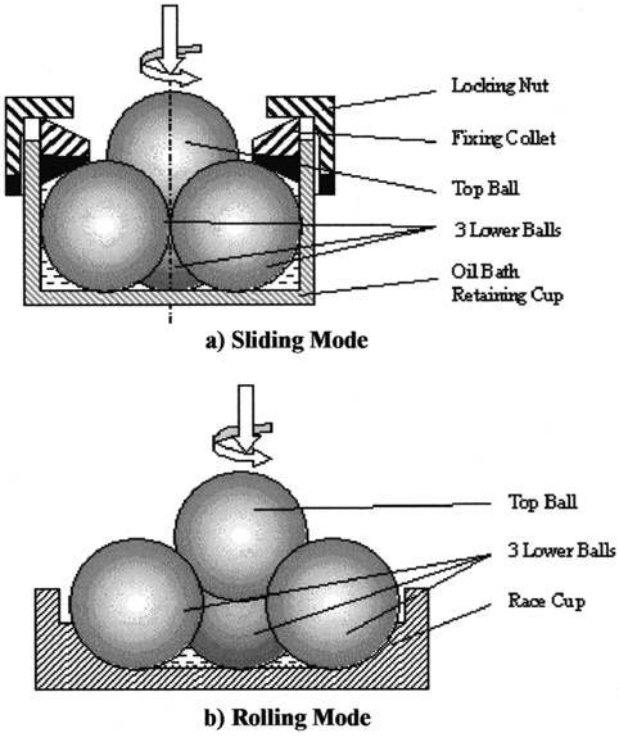


**Fig. 4** Four-ball test cup configurations for sliding and rolling contact

to this spring by means of counterbalance weights to ensure linearity. Movement of the clamp was measured using a capacitance probe, which was linked directly to a data logging computer.

The fusion of vibration, AE and oil debris data for faults generated under conditions representative of US Navy machinery operation was the key goal of the research programme. A test matrix was designed to provide vibration, AE and debris data in speed, load and lubrication regimes closely associated with machinery operation regimes on surface combatants and helicopters. This correlation was important because of the need to fuse sensor data as part of the condition-based maintenance (CBM) technology transition initiative of the US Navy.

These parameters served to define the test conditions for the four-ball machine, which was employed for all tests. The four-ball machine may be used to simulate conditions experienced in a range of machinery operated by the US Navy. Lower loads and speeds are applicable to ship main reduction gearboxes with higher loads and speeds applicable to turbine engine accessory gearboxes.

## 3 DATA ACQUISITION SYSTEM

For maximum diagnostic coverage both vibration and acoustic emission data were collected for post-test analysis. Current machinery diagnostic practice and typical machinery background operational noise spectral content were considered in the selection of the technologies and data acquisition frequency ranges. For typical military and civil air and surface fleet machinery, operational noise spectral content is high in the frequency range, up to about 25 kHz. This range may also contain vibration associated with machinery faults. Because the operating vibration level is often orders of magnitude above vibration signals associated with the types of faults being considered, accurate early detection of faults is difficult and detection reliability is limited. For this reason current diagnostic practice dictates that data should be acquired above 25 kHz to cover the range where machinery operating noise is diminished and the signal to noise ratio for the fault-associated vibration is more favourable. While it would be desirable to collect vibrational data for the full frequency range above the 25 kHz machinery operational noise tail-off, current technology appears to limit reliable linear vibration measurement and the associated calibration standards to the region of 50 kHz.

Acoustic emission was the technology of choice to probe the frequency range above the linear vibration ceiling. For this research, the waveform of the sensor output signal was recorded and analyzed to extract features associated with fault types. The following sections describe the instrumentation selected to implement the acquisition of vibration and AE data.

The data acquisition (DAQ) system used to collect vibration and acoustic emission data consisted of three computer-based subsystems (Fig. 5). Each of the subsystems performed a dedicated task and all were externally connect together to enable synchronization. One computer was used to collect vibration and parametric data channels and two computers were used to collect AE data. A commercial system was used to collect AE hit-based data and a custom system was used to reliably store AE waveform data.

Physical Acoustics Corporation (PAC) acoustic emission transducers were used to convert mechanical energy carried by elastic waves into electrical signals. Two different types of sensors were used: PAC mini30s, with a 300 kHZ resonant frequency and a PAC WD, with a broadband response range of 100 kHz–1Mhz.

The signals from the transducers were connected to individual pre-amplifiers where the signals were given a 40 dB gain and filtered using six-pole Butterworth, band-pass filters with 20 kHz and 1 MHz corner frequencies. Both sensor and pre-amplifier pairs were powered through the shielded coaxial signal cables connected to the main computer.

The PC was fitted with a PAC PCI-DSP board to form a DiSP system. The PCI-DSP board, a four-channel, digital signal processing based AE data acquisition system on a single, full-size, PCI-bus card, was capable of 16-bit, 10 MHz A/D conversion, on-board processing, and included software programmable high pass and low pass filters for each channel. The PCI-DSP also provided the 28 V power supply to the pre-amplifiers and sensors.

Although a standard hit threshold system could be used to detect the large increase in amplitudes

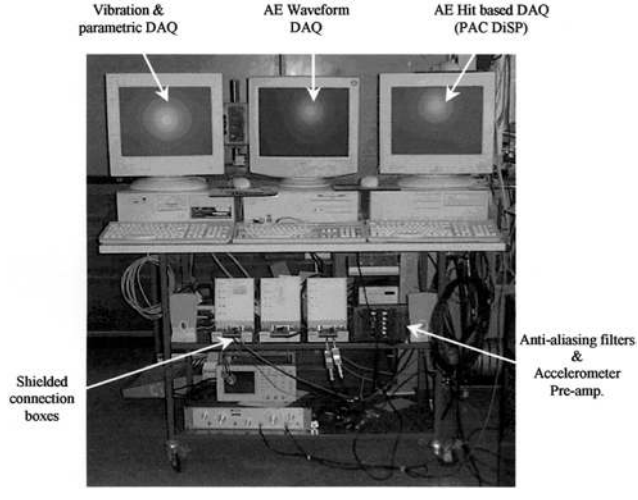


**Fig. 5** Data acquisition system

noticed after pitting had occurred, to monitor the development of a defect required a more continuous solution. A separate computer-based DAQ system was used to reliably record continuous AE waveforms.

The same transducers and pre-amplifiers were used with a T-junction fitted to the output of the pre-amplifiers to allow the signal to be split and used in both AE subsystems.

The outputs from the pre-amplifiers were connected to a shielded connection box via coaxial cables terminated with BNC connectors and DC blockers. The signals had DC components of 28 V, which were removed by passing the signals through 100$\mu$ F capacitors. The shielded connection box was linked to a PC-based DAQ board where the analogue waveform was converted to a digital signal. A NI PCI-6111E DAQ board with a 12-bit resolution and 5 MHz sampling rate per channel was used, allowing accurate representation of the band limited signal. Owing to the high data input rates a SCSI hard disk drive with a spindle speed of 10 000 rpm, capable of 40 Mb/s sustained data throughput, was utilized. Data collection was controlled by custom software and data stored in binary format. The PC specification integrated a 1 GHz processor and 256 MB of memory.

The operating system and software used imposed an upper limit on the size of any one file collected; due to the 32-bit file structure a file larger than 2 GB cannot exist. This limited continuous AE waveform collection to approximately 2 minutes with two-channels sampled at 5 MHz. To monitor longer duration tests required non-continuous AE waveform collection. To achieve this, one complete revolution of data was collected every 2.5 seconds.

## 4 RESULTS

A comprehensive test programme was undertaken; tests were conducted using load and speed ranges representative of conditions experienced within US naval air and surface combatants. It is impractical to display all the results in this paper, so only a selection of tests that display trends noted across the spectrum of tests is shown. More results can be found in references [**14**–**16**].

### 4.1 Sliding tests

Sliding tests were conducted using a range of different loads and speeds. At lower loads the four-ball machine would run in a stable state, without transitions between lubricating regimes. When the pressure in the contact is low enough for the film thickness to be sustained by the lubricant, scuffing does not occur.

At higher loads, shortly after starting the machine the lubricant film would fail, causing metal-to-metal contact. As the surfaces of the three lower balls abrade at their respective contact points, the contact area increases and thus the contact pressure decreases. Eventually the pressure falls to a level where lubricant can re-enter the contact and scuffing wear stops. Owing to the increased area of the lubricated contact, friction in the system after the seizure event is higher than before.

The load at which scuffing will occur is dependent on the properties of the lubricating oil. With the oil used in these tests, the transition load is approximately 63 kg. A typical friction trace for a test conducted at a load above the transition load is shown in Fig. 6. This test (Test 1) was conducted at a load of 80 kg and speed of 1500 rpm.

There is a short period of running-in followed by low friction. The transition into seizure is sudden, causing a sharp increase in fiction. During recovery from seizure the friction in the system drops; however, friction remains slightly higher than before seizure. The amplitude shown on the graph is voltage as output from the capacitance probe amplifier and is proportional to the friction force in the contact.

Acoustic emission data were collected continuously during sliding tests, the duration of each typically being 60 seconds. The continuous data file was broken into smaller segments using signals recorded from the shaft position encoder. Each new segment file contained data from one revolution of the upper ball. For a 60-second test with a spindle speed of 1500 rpm, 1500 files would be created. To limit the size of the result file and decrease the processing time required, not all of these files were processed together.

With acoustic emission waveforms the quantity of data collected proved troublesome to deal with.

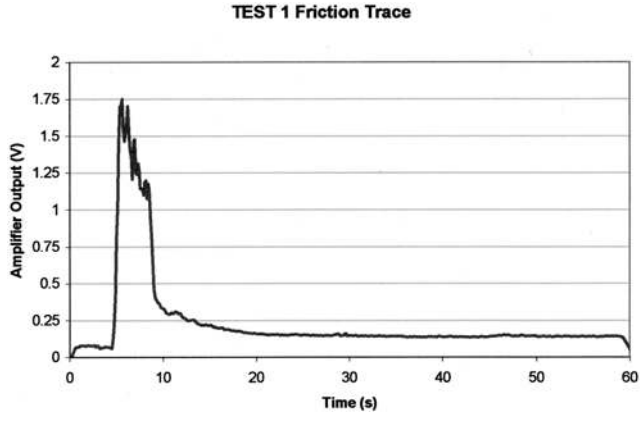


**Fig. 6** Typical sliding test friction trace

While statistical processing was capable of considerable data reduction, to retain good resolution in the frequency domain large matrices of data were necessary. These matrices contain too many points to be loaded into the likes of Microsoft Excel, so were instead displayed as intensity plots generated by a simple LabVIEW program.

Figure 7 shows how the RMS of the broadband AE signal varied throughout Test 1. From the set of 1500 files, only every third file was processed, giving a time resolution of three revolutions or 0.12 seconds. The raw waveform was digitally filtered with a pass-band between 100 and 408 kHz before further processing.

The RMS values exhibit a good correlation with the friction trace shown earlier. The large difference in values between fault/no fault states shown here is suitable for simple alarm level monitoring systems.

The figures that follow present the frequency domain analysis results for Test 1. For the frequency domain analysis, 250 files were processed, giving a time resolution of six revolutions or 0.24 seconds. Only data collected by the broadband transducer, PAC WD (channel 2), are shown.

The results file matrices were plotted on intensity graphs, giving a time–frequency representation of the test. The $x$-axis indicates time, in seconds, from the start of the test. The $y$-axis denotes frequency, in Hertz. Amplitude data are plotted on the $z$-axis, and are represented by the colour of the ($x$, $y$) point, denoted by the full spectrum colour scale shown at the right of each graph.

Figure 8 displays the FFT results for the frequency range 0–1 MHz. Figures 9 through 11 display the same data with the axes adjusted to show zoomed views of the frequency bands 0–50kHz, 50–150 kHz and 150–250 kHz, respectively.

Figure 8 shows the response on the sensor over its entire operating range. The seizure event, occurring between 5 s, and 9 s, is clearly visible from the sharp increase in amplitude of all peaks. Signal amplitudes before seizure are also less than after seizure. The correlation between AE amplitude and friction is good at all peaks in the frequency plot.

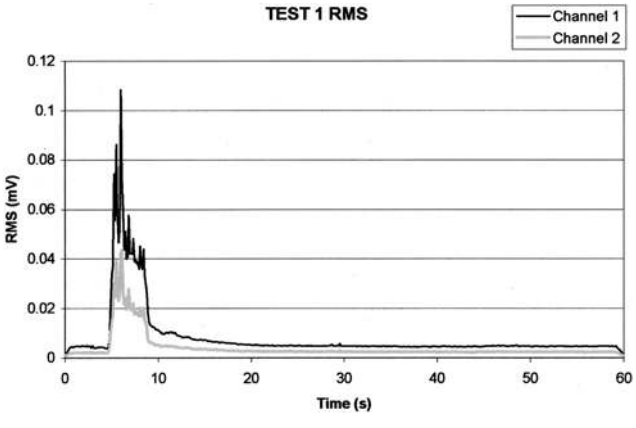


**Fig. 7** Sliding test RMS results, Test 1

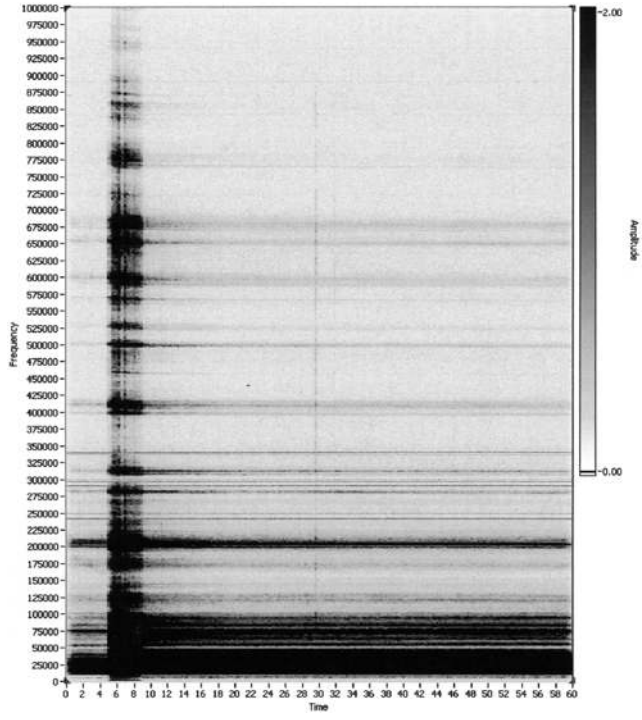


**Fig. 8** Sliding test FFT results, Test 1, 0–1 MHz

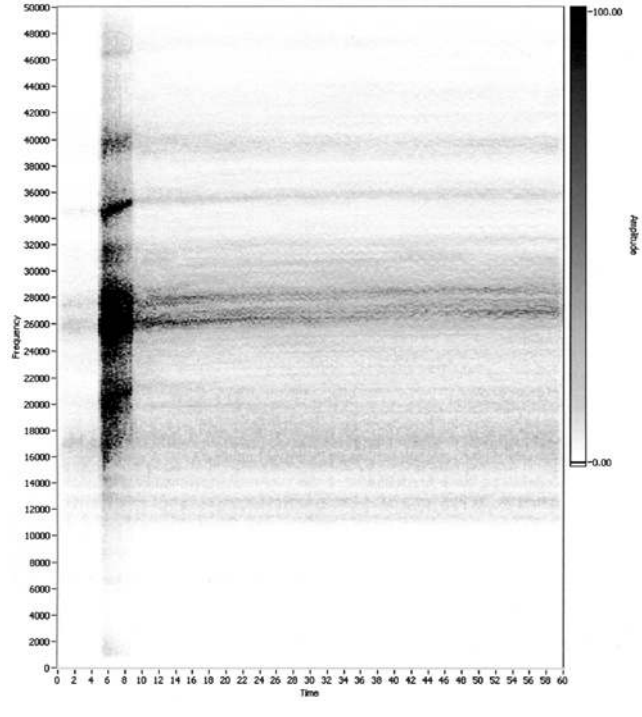


**Fig. 9** Sliding test FFT results, Test 1, 0–50 kHz

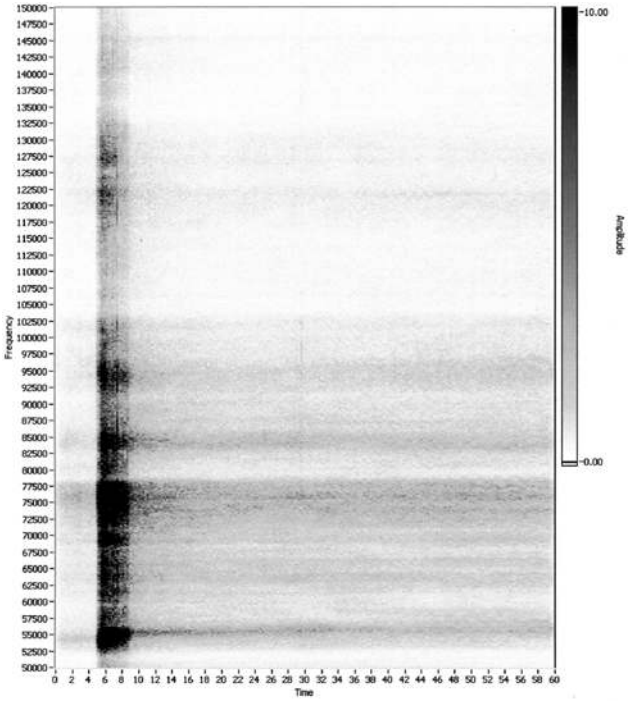


**Fig. 10** Sliding test FFT results, Test 1, 50–150 kHz

The low-frequency AE response is similar to that observed during vibration monitoring; during seizure the frequency of the peaks increases. This is most clearly seen between 34 and 35 kHz in Fig. 9. (Vibration monitoring results can be found in the references cited at the start of this section.)

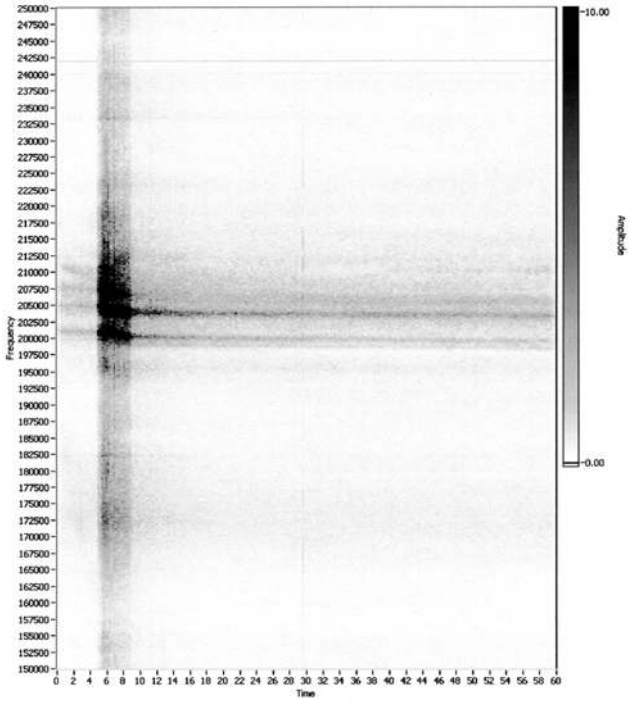


**Fig. 11** Sliding test FFT results, Test 1, 150–250 kHz

Peaks in the FFT data continue to exhibit a tendency to increase in frequency during seizure up to approximately 100 kHz (Fig. 10). Peaks above 100 kHz exhibit the opposite effect; during seizure these peaks reduce in frequency (Fig. 11). At even higher frequencies, up to 1 MHz, although the amplitude of the signal is less, the same decreasing frequency phenomenon is still observed.

To try and ascertain the reason for this behaviour, the test balls were subjected to an extensive post-test autopsy. The wear scar on one lower ball, resulting from scuffing wear, is shown in Fig. 12. Striations can be seen, indicating the direction of relative motion between the contacting surfaces. The dimensions of the wear scars are dependent on load and lubricant quality. The size of the wear scar will also be proportional to the quantity of wear particles generated.

Figure 13 depicts the wear track on the top ball from the same sliding test. Some metal-to-metal transfer, from the lower balls to the top ball, can be seen. High temperatures in the contact cause localized welding and adhesion, metal is then torn off the lower balls by the relative motion in the contact.

After examining the wear scars, balls from some of the tests were mounted in conductive resin and sectioned through the wear scars. The exposed surface was then polished to a mirror finish using progressively finer polishing pastes. The sectioned balls were examined using a scanning electron microscope (SEM). No subsurface cracks were found. Further compositional analysis revealed no change around the contact area.

The sectioned surface was then etched using Nital, to enhance the grain structure and make the specimen suitable for optical microscopy. The Nital contained 10 per cent concentrated nitric acid in solution with water. Figure 14 is a view of the section

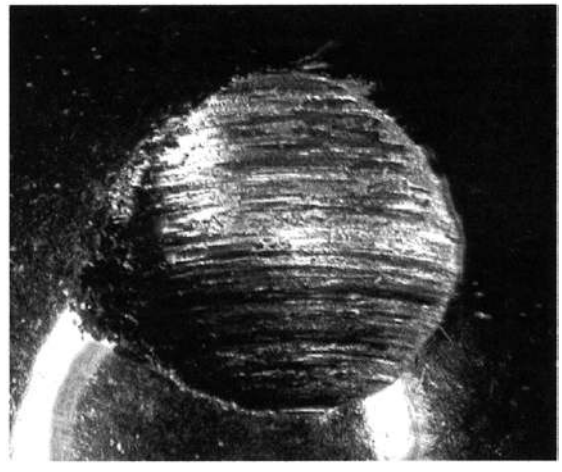

**Fig. 12** Sliding test lower ball wear scar

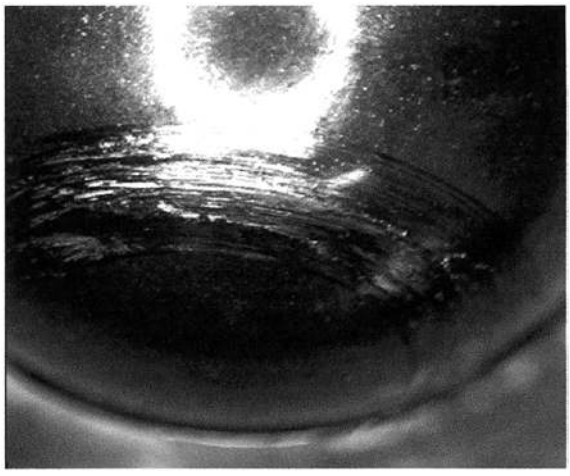

**Fig. 13** Sliding test top ball wear track

**Fig. 15** Sliding test wear scar, 100 ×

through the wear scar, magnification 50×. Figure 15, magnification 100×, shows more closely the white transfer layer and deformation at the edge of the wear scar. The discolouration in the area of the wear scar could be indicative of work hardening or temperature effects, although no difference in hardness could be detected through microhardness testing.

### 4.2 Rolling tests

Four-ball rolling tests were conducted at loads of 500, 600, 700 and 800 kg with speeds of 1500 and 2500 rpm. Throughout the test program the data acquisition system was periodically revised to improve the quality of the data collected. Owing the long durations of rolling tests, data could not be collected continuously, as in the sliding tests. Initially the DAQ system was configured to collect bursts of data at specified intervals, data capture being triggered directly from timing pulses generated in the vibration subsystem. Later, the system was improved by triggering data capture from pulses generated by the shaft position encoder, only after a specified wait period had passed. This ensured that the first data point in each file corresponds to the same shaft position.

The four-ball machine was set up and run until a pit could be detected audibly. The cyclic loading on each ball causes the material to fatigue. Cracks will develop beneath the surface of the ball and propagate towards the surface, where a pit will form.

The following results were obtained by processing data collected with the later DAQ system. The time interval between data files, or trigger wait period, was set at 2.5 seconds. Only results from two tests (Test 2 and Test 3) are included here. These tests were both conducted at 1500 rpm with a load of 800 kg.

Throughout all tests, one complete revolution of data (40 ms at a speed of 1500 rpm) was collected every 2.5 seconds. The $x$-axis on all results graphs indicates the time, in seconds, from the start of the test. The $y$- and $z$-axes are as described for the sliding tests.

Figures 16 and 17 show the RMS history of the broadband AE signal. The raw waveform was digitally filtered with a pass-band between 100 and 400 kHz before further processing. RMS values for both tests steadily decrease until failure, where the values increase by an order of magnitude. The initial ramp up of values at the start of tests is consistent with machine spindle run-up and the slow addition of load, which occur at the start of each test. Although pitting can be detected using these methods, pitting cannot be predicted due to the lack of precursory events.

The following figures show the frequency plots for the same two tests. These tests were chosen to indicate two main trends that have been identified

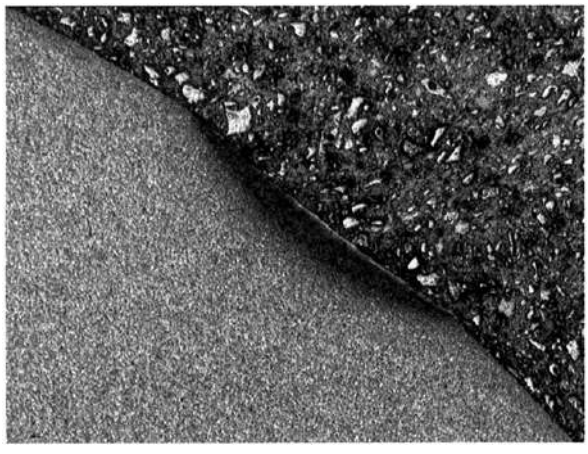

**Fig. 14** Sliding test wear scar, 50 ×

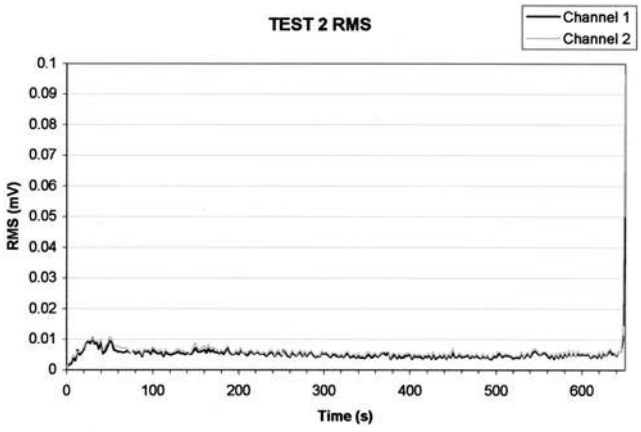


**Fig. 16** Rolling test RMS results, Test 2

from across the range of tests conducted. Each test is presented as a set of three plots. The first graph shows the response of the sensor over its entire operating range, while the next two show zoomed views of the areas of interest.

Figure 18 displays the FFT results from Test 2, for the frequency range 0–1 MHz. Most of the activity is at lower frequencies. Figures 19 and 20 display the same data with the axes adjusted to show zoomed views of the frequency bands 50–150 kHz and 150–250 kHz, respectively.

In the frequency range 50–150 kHz there is a noticeable drop in amplitude of the peaks starting at 90 kHz and 117.5 kHz. All peaks also experience a small reduction in freqency throughout the test.

Some very interesting trends are displayed between the frequencies of approximately 180 kHz and 230 kHz. All tests that exhibited the early spectral behaviour shown above ended with the same strong pulsing also shown.

Figure 21 displays the FFT results from Test 3, for the frequency range 0–1 MHz. Figures 22 and 23 display the same data with the axes again adjusted

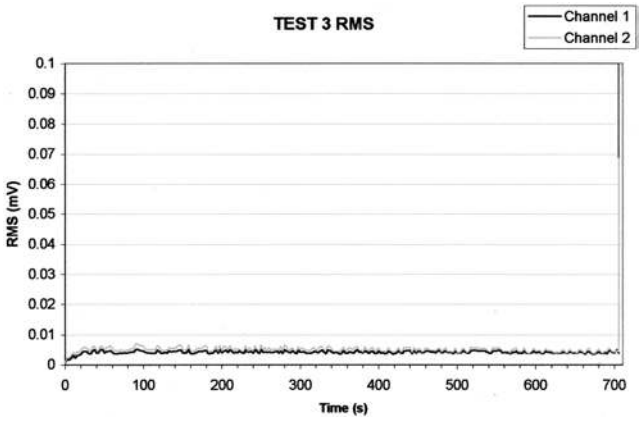


**Fig. 17** Rolling test RMS results, Test 3

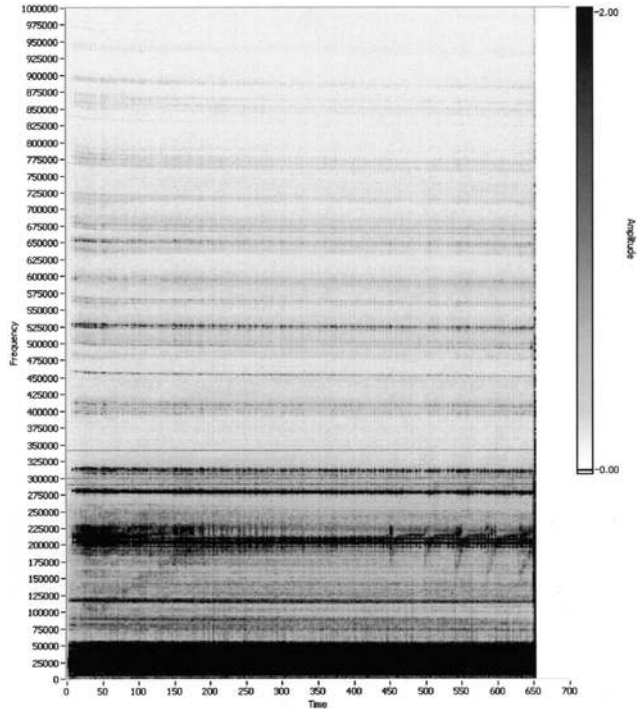


**Fig. 18** Rolling test FFT results, Test 2, 0–1 MHz

to show zoomed views of the frequency bands 50–150 kHz and 150–250 kHz, respectively.

The overall picture for Test 3 is similar to Test 2, but no closer inspection different trends are discovered. In Fig. 22, a distinct shift of energy between

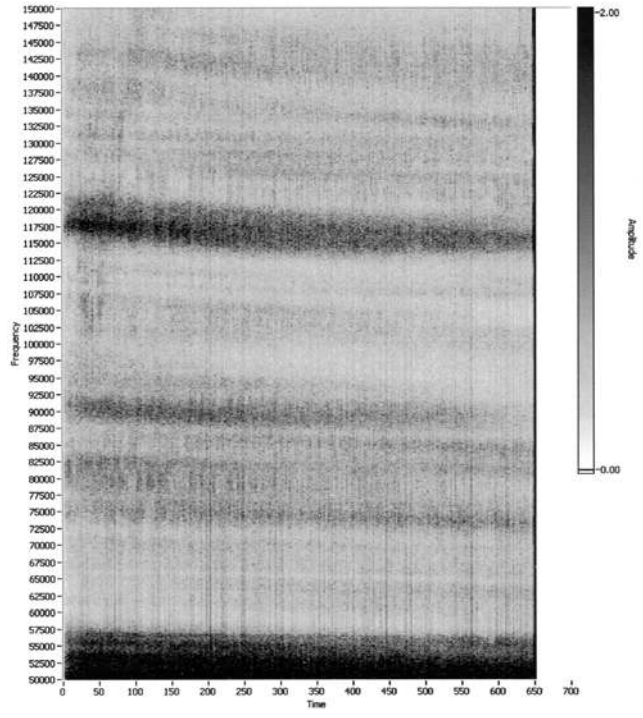


**Fig. 19** Rolling test FFT results, Test 2, 50–150 kHz

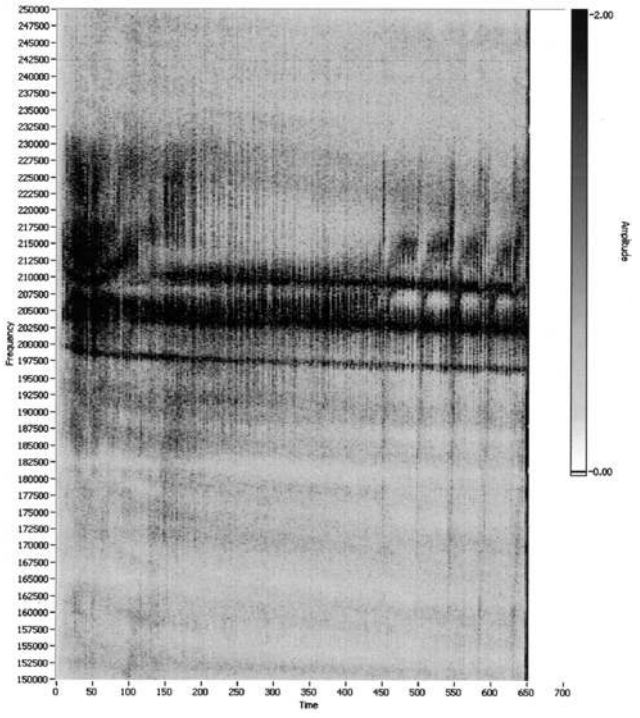


**Fig. 20** Rolling test FFT results, Test 2, 150–250 kHz

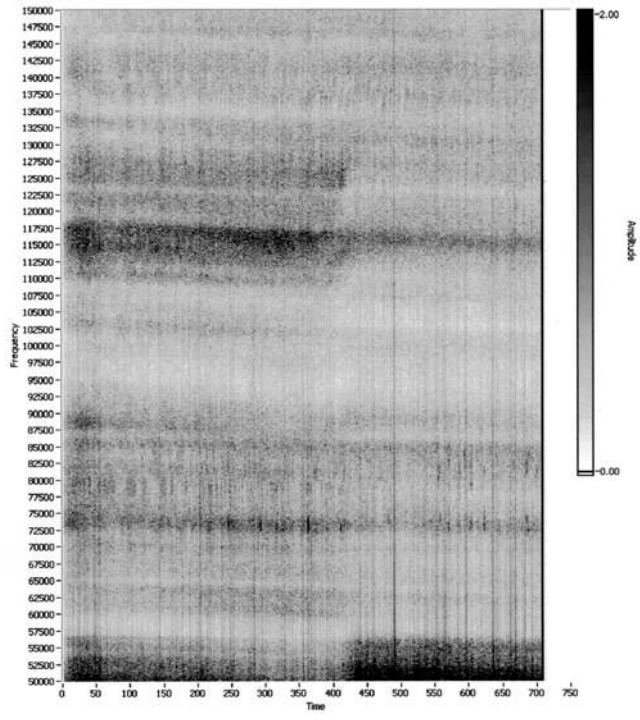


**Fig. 22** Rolling test FFT results, Test 3, 50–150 kHz

the peak at 115 kHz and the peak at 50 kHz occurs at time 420.

The frequency content between 150 kHz and 250 kHz is similar to Test 2, except the pulsing energy is more evenly spread throughout the test.

Another point to note is that throughout the tests all frequency peaks undergo a negative shift of approximately 5 per cent. This is most noticeable in Fig. 20; the frequency of the three peaks can be seen to drop as the test progresses.

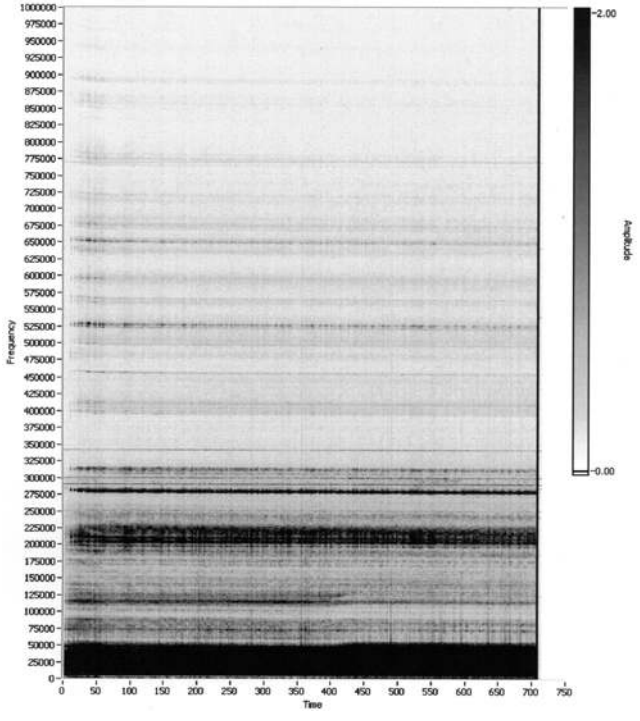


**Fig. 21** Rolling test FFT results, Test 3, 0–1 MHz

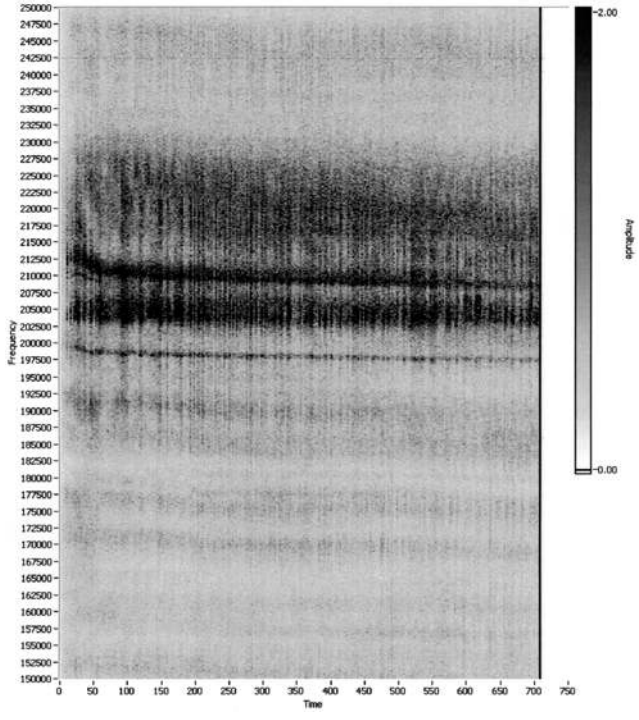


**Fig. 23** Rolling test FFT results, Test 3, 150–250 kHz

A typical pit resulting from rolling tests is shown in Fig. 24. The pit is approximately 1 mm in diameter and 0.5 mm deep. This matches the Timken criterion for removal of a bearing from service.

After examining the surfaces of the balls, some were sent to the Fuels and Lubricants division at QinetiQ where they were mounted in conductive resin and sectioned through their pit. The exposed surface was then polished to a mirror finish.

The sectioned balls were examined using a scanning electron microscope. Subsurface cracks were found. Further compositional analysis revealed no change around the damaged areas. Figure 25 is an SEM micrograph of a rolling test upper ball, showing the section through the pit. Crack networks that would eventually result in wear particle generation can clearly be seen.

After SEM analysis the sectioned balls were etched and examined optically. Figure 26 is a view of a pit taken at 50× magnification. With a higher magnification, two crack propagation modes are visible: intergranular and transgranular. Transgranular cracking, through grain boundaries, produces straight edges while intergranular cracking, along grain boundaries, produces jagged edges.

There were no signs of persistent slip bands caused by cyclic fatigue or any other forms of work hardening. Micro hardness testing failed to find an appreciable difference across the section of the ball.

In an attempt to find the cause of the trends defined above, a LabVIEW program was constructed to process data by FFT in real time. As soon as events were spotted on screen the tests were stopped.

Test 4 was terminated due to the presence of pulsing at frequencies between 210 and 230 kHz. Test 5 was terminated due to the presence of an energy shift between the peak centred at 112.5 kHz and the peak at 50 kHz. The test balls were examined offline at QinetiQ, where subsurface cracks were found in the absence of any surface failure. The subsurface cracks discovered from these tests are shown in Figs 27 and 28. If these tests were allowed to continue, pitting would have initiated in the area of the subsurface cracks.

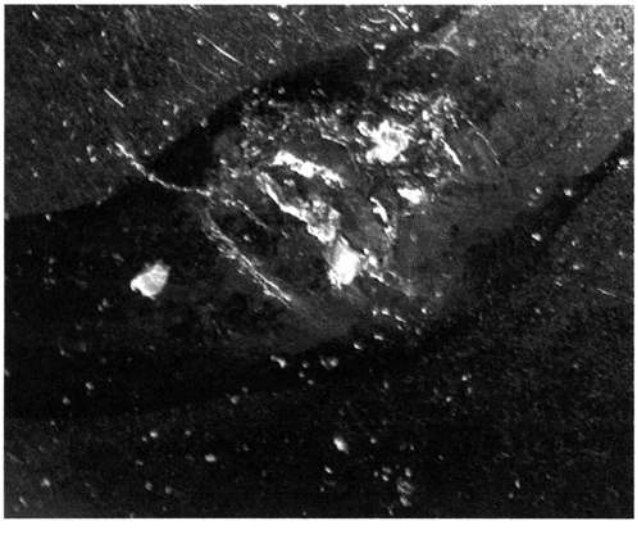

**Fig. 24** Rolling test top ball pit

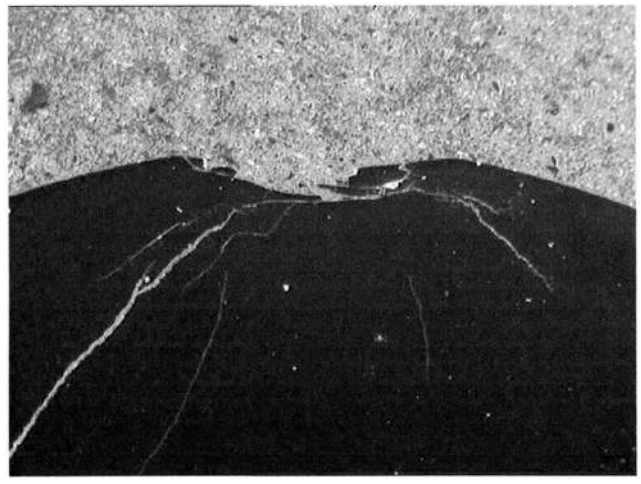

**Fig. 25** SEM micrograph showing pit and subsurface crack networks

## 5 DISCUSSION

Tests were conducted to simulate two wear modes commonly experienced by gear and bearing components in naval air and surface combatants. Scuffing wear results from collapse of the lubricant film in the contact. When the pressure in the contact is greater than that which the lubricant can sustain, metal-to-metal contact occurs. Scuffing wear events can occur due to either poor lubrication, degradation

**Fig. 26** Subsurface crack close to pit

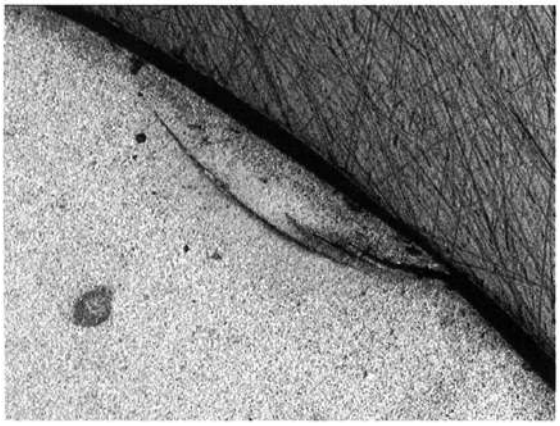

**Fig. 27** Subsurface crack from Test 4

of the lubricant over time, excess load or a change in lubricant properties from temperature effects or foreign additives. Fatigue wear takes place when material is subjected to cyclic loading. Material properties will change over time as a result of repeated load variations. In bearing applications, the metal will suffer ductility exhaustion. As the metal becomes more brittle, subsurface cracks form and propagate towards the surface, leading to removal of metal from the surface. Both scuffing wear and pitting fatigue wear can be generated using the four-ball machine, which can be configured for either sliding or rolling operation, respectively.

Wear debris analysis is a proven technique for classification of wear modes. By optically examining the topography of particles generated by machinery, the modes of wear experienced can be determined. Particles produced by scuffing wear have markedly different characteristics from those produced by fatigue. Sets of wear particle attributes have been established that correspond to specific wear modes. Oil analysis is usually conducted off-line at regular service intervals over machine life, giving poor time resolution for fault detection. LaserNet Fines is a recent development from US Navy research programmes. LaserNet Fines is an on-dine oil analysis tool. Particles in the oil flowing through its test cell are photographed and analysed automatically to extract key features and identify the wear mode.

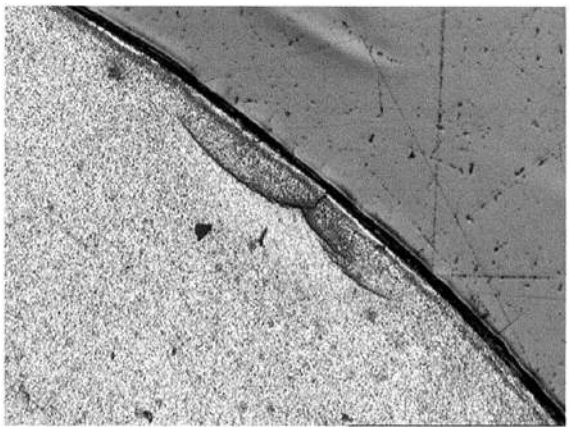

**Fig. 28** Subsurface crack from Test 5

The aim of this research programme was to identify any high-frequency feature vectors indicative of different fault types, which could be fused with LaserNet Fines feature vector sets to produce a more reliable machinery health monitoring system. Throughout tests, vibration, acoustic emission and wear debris data were collected. Vibration waveforms were collected to assess the effectiveness of extending the condition monitoring bandwidth up to 50 kHz. The acoustic emission technique was used to probe the frequency range over 50 kHz.

Results from four-ball sliding tests indicate that both AE and vibration signal amplitudes respond well to changes in contact friction. Vibration frequency spectrum peaks appear at approximately 17 and 32 kHz during the seizure event. The signal-to-noise ratio at these frequencies is higher than at lower frequencies. During seizure the frequencies of these two peaks increase by approximately l kHz. The mass of metal worn away from the surface of the balls during the seizure event is insufficient to account for this degree of change. Localized changes in the system at the contact areas cause the stiffness to increase.

Lower frequency AE signals exhibit similar trends to vibration signals. Peaks in the FFT of AE signals up to 100 kHz undergo a positive frequency shift. Higher frequency AE shows the opposite behaviour; peaks over 100 kHz undergo a negative shift in frequencies. This convergence of frequencies during seizure could be due to any, or all, of the changes that were observed by the post-test autopsy. Metal transfer between balls, loss of mass from the lower balls, heating effects in the vicinity of the contact and contact area changes, which would cause global stiffness changes, were all evident after inspection of the surface and cross-section of the balls.

As AE is responsive to scuffing, a simple alarm level monitoring system, based on AE RMS of the broadband signal could be used. However, different information is held within different frequency bands.

Results from four-ball rolling tests show that both high-frequency vibration and AE signals can be used to detect pitting. Signal levels generated during normal running have low amplitudes. Once pitting has occurred, impulses generated as the pit periodically passes through the contact excite multiple resonances, causing the RMS amplitude of both sets of

data to increase by an order of magnitude. Closer inspection of acoustic emission data reveals changes in signal content prior to pitting. Several interesting trends have been noted and are described briefly here. There are many peaks in the FFT of AE signals. Over the duration of a test, these peaks all suffer a small drop in frequency (typically 5 per cent). The majority of these peaks also slowly decrease in amplitude during tests. In key frequency bands, differences were noted between tests.

Across the range of tests conducted, two main differences were noted. Before pitting had occurred, some tests exhibited a distinct shift of energy from a peak at approximately 115 kHz to a peak at approximately 50 kHz. This typically occurred between 40 and 80 per cent of the test ball fatigue life. Other tests showed patterns of activity between the approximate frequencies of 180 and 230 kHz. Distinct pulsing characteristics could be seen shortly before pitting. Various signal processing techniques were used to remove unwanted noise from the data. The spectral density of the signal can be used to give a low noise representation of the frequency content. Two sensors with different frequency responses were used on all tests. To highlight source events and remove sensor response dependencies, the cross-correlation was computed between channels. The FFT history of the cross-channel correlation results contained similar information. All of the trends previously seen were still present. This indicates that peaks in signal FFT must be due to machine resonances or representative of the frequency of the AE source.

Post-test autopsy of the balls showed subsurface crack networks leading to the pits, the severity of which were dependent on the test load. How cracks propagate to cause a pit and allow wear particle generation could also be seen.

To establish the cause of the change in frequency patterns observed before pitting, software was developed to allow real-time display of the FFT processing results. Balls used in tests that were terminated due to trends observed on-screen were found to possess no surface damage but did contain subsurface cracks. Therefore, an automated pattern recognition system based on AE time-frequency data could be used for on-line detection of subsurface cracking. Acoustic emission monitoring is capable of detecting wear events prior to either vibration monitoring or wear debris analysis techniques.

Further work needs to be conducted to identify the cause of crack initiation that relates to each trend. Further investigation also needs to be completed to establish why peaks are seen at the particular frequencies noted. If these frequencies are not system resonances, but frequencies associated with AE sources, the number of different sources must be identified. Testing on a wider range of machinery should be conducted to compare results.

## 6 CONCLUSIONS

A complex array of physical emerges from the behaviour monitored in the tests. Three feature are apparent however.

1. Scuffing wear can be easily detected by AE with a high signal-to-noise ratio.
2. Pitting is also easily detected using AE, again with a good signal-to-noise ratio.
3. It is also possible to measure a precursor to pitting by the detection of the subsurface cracks that later lead to pitting.

## ACKNOWLEDGEMENTS

The authors wish to acknowledge the funding and support provided by the Naval Research Laboratory and the Office of Naval Research and also the help of T. J. Nowell at QinetiQ with the metallurgical analyses.

## REFERENCES

1 **Holroyd, T.** *Acoustic Emissions and Ultrasonics*, 2000 (Coxmoor Publishing Company, Oxford).
2 **Ikeda, T.** *Fundamentals of Piezoelectricity*, 1990 (Oxford University Press, Oxford).
3 **Drouillard, T.** A history of acoustic emission. *J. Acoustic Emission*, 1996, **14,** 1–33.
4 **Tandon, N.** and **Choudhury, A.** A review of vibration and acoustic emission measurement methods for the detection of defects in rolling element bearings. *Tribology Int.*, 1999, **32,** 469–480.
5 **Reeves, C.** *Vibration*, 2000 (Coxmoor Publishing Company, Oxford).
6 **Williams, R.** *Acoustic Emission*, 1980 (Adam Hilger Ltd, Bristol).
7 **Li, X.** A brief review: acoustic emission method for tool wear monitoring during turning. *Int. J. Machine Tools & Manufacture*, 2002, **42,** 157–165.
8 **Dimla Snr, D.** Sensor signals for tool-wear monitoring in metal cutting operations—a review of methods. *Int. J. Machine Tools & Manufacture*, 2000, **40,** 1073–1098.
9 **Li, C. J.** and **Li, S. Y.** Acoustic emission analysis for bearing condition monitoring. *Wear*, 1995, **185,** 67–74.
10 **Shiroishi, J., Li, Y., Liang, S., Kurfess, T.,** and **Danyluk, S.** Bearing condition diagnostics via vibration and acoustic emission measurements. *Mech. Syst. Signal Proc.*, 1997, **11,** 693–705.
11 **Heng, R.** and **Nor, M.** Statistical analysis of sound and vibration signals for monitoring rolling element bearing condition. *Appl. Acoustics*, 1998, **53,** 211–226.

12 **Choudhury, A.** and **Tandon, N.** Application of acoustic emission technique for the detection of defects in rolling element bearings. *Tribology Int.*, 2000, **33,** 39–45.
13 *Methods for Analysis and Testing, Vol. 2, Methods IP 262 to 376*, 1986 (John Wiley and Sons).
14 **Price, E. D., Sperring, T. P., Roylance, B. J., Lees, A.W.,** and **Friswell, M. I.** Sensor fusion for condition monitoring. *Proc. Int. Conf. on Condition Monitoring*, 2001, Oxford.
15 **Price, E. D., Lees, A. W.,** and **Friswell, M. I.** *Application of High Frequency Monitoring for Classification of Rolling Element Bearing Failures*, 2001 (DAMAS, Cardiff).
16 **Price, E. D.** High frequency techniques for condition monitoring. PhD thesis, University of Wales, Swansea, 2002.